Scientific Inquiry and Review (SIR)
Volume 6 Issue 1, Spring 2022
ISSN $_{(P)}$: 2521-2427, ISSN $_{(E)}$: 2521-2435
Homepage: https://journals.umt.edu.pk/index.php/SIR

Article QR

Title: **Implementation of Lengyel-Epstein Reaction Model for Zinc Oxide (ZnO) Nanostructures by Comparing Euler and Fourth-Order Runge–Kutta (RK) Methods**

Author (s): Kaniz Fatima[1], Basit Ali[2], Mahnoor[3]

Affiliation (s): [1]Department of Humanities & Social Sciences, Bahria University, Karachi, Pakistan
[2]Department of Electrical Engineering, Bahria University, Karachi, Pakistan
[3]DOW University of Health Sciences, Karachi, Pakistan

DOI: https://doi.org/10.32350/sir.61.02

History: Received: November 01, 2021, Last Revised: January 16, 2022, Accepted: March 17, 2022, Published Online:

Citation: Fatima K, Ali B, Mahnoor. Implementation of lengyel-epstein reaction model for Zinc Oxide (ZnO) nanostructures by comparing euler and fourth-order Runge–Kutta (RK) methods. *Sci Inquiry Rev.* 2022;6(1):23-33. https://doi.org/10.32350/sir.61.02

Conflict of Interest: Author(s) declared no conflict of interest

A publication of
School of Science
University of Management and Technology, Lahore, Pakistan

Implementation of Lengyel-Epstein Reaction Model for Zinc Oxide (ZnO) Nanostructures by Comparing Euler and Fourth-Order Runge–Kutta (RK) Methods

Kaniz Fatima[1], Basit Ali[2*] and Mahnoor[3]

[1] Department of Humanities & Social Sciences, Bahria University, Karachi, Pakistan
[2] Department of Electrical Engineering, Bahria University, Karachi, Pakistan
[3] DOW College of Pharmacy, DOW University of Health Sciences, Karachi, Pakistan

*basitali.bukc@bahria.edu.pk

Abstract

The current study presents Lengyel-Epstein reaction model for the analysis of the reaction kinematics of the growth of Zinc oxide (ZnO) nanostructures using the fourth-order Runge-Kutta (RK) method. The aim is to propose an improved approximation technique for the computation of the concentrations of Zinc ion and Hydroxyl ion. For this purpose, a comparison of Euler's method with the fourth-order RK method was made to gauge their effectiveness in determining the concentrations of both ions. It was determined that the fourth-order RK method gives more stable results than Euler's method. In this regard, the comparison with Euler's method showed that the rate of convergence of the RK method is more appropriate than Euler's method. Furthermore, it was also determined that the RK method validates the experimental results for the formation of ZnO nanostructures using the aqueous chemical growth (ACG) method.

***Keywords*:** Aqueous Chemical Growth (ACG) method, Euler's method, Lengyel-Epstein reaction model, nanostructures, fourth-order Runge–Kutta (RK) method, Zinc Oxide (ZnO)

Introduction

Zinc oxide (ZnO), a natural inorganic compound, has a wide variety of applications in the modern technological world. It is usually found in (white) powder form and remains insoluble in water, although it is soluble in dilute acids and bases. The particle size of ZnO is less than 100 nm. The solubility level of ZnO is also very low, that is, about 1.6–5.0 mg/L [1].

The physical and chemical properties of the nanoparticles of ZnO distinguish it from other metal oxides. It is used in various industries and for the preparation of various industrial products, such as glass, paint, optical materials, rubber, plastic, batteries, coating, and cosmetics. The use of ZnO nanoparticles is also widespread in the biomedical field, especially in the anticancer and antibacterial subfields. This is due to the fact that ZnO has a strong ability to generate excessive reactive oxygen species (ROS) and discharges Zinc ions. Furthermore, ZnO nanoparticles can also act as anti-diabetic because zinc has the ability to maintain the level of insulin [2, 3].

ZnO is defined as a semiconductor that has the distinctive properties of electric conductivity, photosensitivity, chemical sensing, and piezoelectricity. Due to these characteristics, ZnO nanoparticles have a strong room temperature luminescence, a high exciton binding energy (60 meV), and a wide band gap of 3.4-3.7 eV [4]. These nanoparticles are good ultraviolet absorbers; therefore, they are used in skin lotions and creams for UV protection. They are also used in ointments intended for wound healing and to get relief from swelling. In addition to these essential biomedical properties, they have excellent drug carrier systems. Moreover, the US Food and Drug Administration (FDA) has marked ZnO as a GRAS (generally recognized as safe) substance and ZnO nanoparticles that are larger than 100 nm are supposedly biocompatible [5, 6].

Due to the wide range of applications of ZnO nanoparticles, it is very important to produce ZnO in a huge amount. ZnO nanostructures can be produced easily by using different approaches at low temperatures, such as the Sol-Gel method, chemical-bath deposition method, self-combustion method, and aqueous chemical growth method. Among all these, the most common and highly result-oriented method is the aqueous chemical growth (ACG) method. This method can produce various morphologies of ZnO nanostructures including nanorods, nanotubes, nanowires, nano flexes, nanospheres, and nanoneedles by optimizing growth parameters. These morphologies of ZnO have drawn considerable interest because of their exceptional qualities, such as their low manufacturing cost, non-toxicity, ease of fabrication, superior biological compatibility, high electron transfer rates, and enhanced analytical performance [7-9].

The growth of ZnO nanostructures can be measured via a mathematical model known as Lengyel-Epstein reaction model. In this model, Euler's method is used to predict the growth of ZnO nanostructures [4]. In this paper, the Runge-Kutta (RK) fourth-order method is used to predict the growth rate of the concentration of Zn ions and Hydroxyl ions.

To estimate the growth rate of ZnO nanostructures analytically, the Euler integration method is used as the elementary method. It has two types of errors, that is, truncation error and cumulative error. These errors affect the accuracy up to a certain level. The most often used technique for ODE numerical solutions is the Runge-Kutta integration method. The advantages of this integration method include its simplicity in terms of programming and the stability of the estimation. However, this approach necessitates a more complex calculation as compared to the previously used integration technique. In the fourth-order RK method, the truncation error is O (h^3) and the cumulative error is O (h^2), which shows the stability of this integration method as compared to the Euler's method [10].

2. Experimental Procedure

For the growth of ZnO nanoparticles, a contamination-free environment is needed. This is because in the ACG method, the procedure can be influenced by the surrounding environment. In this method, an uncontaminated gold coated glass is used as a substrate. Before the beginning of the experiment, the gold coated glass was dipped into a solution of hydrofluoric acid which had low concentration. After a few minutes, it was washed with acetone and dried with the substrate with nitrogen gas at room temperature. Then, the actual process started with the spin coating technique. At 4500 rpm, a solution of Zinc acetate dihydrate was spun and coated on the substrate 3-4 times. The substrate was kept at 70^{o}C for a few minutes to settle down the solution.

A solution was prepared in a container by taking Zinc nitrate and hexamethylenetetramine with 1:1 concentration and adding it to 250 ml of DI water. Then, we dipped the seed coated substrate into the prepared solution using the holder. Afterwards, the container was placed in an oven for 7 hours, which was preheated at 100^{o}C. After 7 hours, the oven was turned off and left for 30 minutes to cool down. Then, we separated the substrate from the holder [11-13]. A layer of ZnO nanorods was obtained. After changing the pH of the solution by mixing it with 25% ammonia, ZnO nanowires were obtained.

3. Chemical Reactions to Form Zinc Oxide

For the formation of ZnO, two types of ions are required. The first is Zinc ion (Zn^{+2}) and the other is Hydroxyl ion (OH^-). Zn^{+2} can be obtained from metal salt after the decomposition of Zinc nitrate [14].

$$Zn(NO_3)_2.6H_2O + 6H_2O \rightarrow Zn^{+2} + 2NO_3^-,$$

OH^- can be formed after the hydrothermal decomposition of HMT.

$$(CH_2)_6N_4 + 6H_2O \rightarrow 6HCHO + 4NH_3,$$

$$NH_3 + H_2O \rightarrow NH_4 + OH^-.$$

After the deposition of both the ions, ZnO can be formed.

$$2OH^- + Zn^{+2} \rightarrow Zn(OH)_2,$$

$$Zn(OH)_2 \rightarrow ZnO\ (s) + H_2O.$$

4. Mathematical Model

Euler's method is used as a numerical method to approximate the results in [4]. However, in this paper, Runge-Kutta's fourth-order method is used to approximate the growth of Zinc ion and Hydroxyl ion. The equations used to construct the model are as follows:

$$NH_3 + H_2O \rightarrow NH_4^+ + OH^-, \quad (1)$$

$$Zn(NO_3)_2.6H_2O + 6H_2O \rightarrow Zn^{+2} + 2NO_3^-, \quad (2)$$

$$2OH^- + Zn^{+2} \rightarrow ZnO + H_2O. \quad (3)$$

Differential equations using Lengyel-Epstein reaction model constructed in [4] are as follows:

$$\frac{dx}{dt} = f(x,y) = a_1 - x - 4\left(\frac{xy}{(1+x^2)}\right),$$

$$\frac{dy}{dt} = g(x,y) = a_2 x\left(1 - \frac{y}{(1+x^2)}\right),$$

where x and y represent the concentrations of $OH^-$and Zn^{+2}, respectively.

The proposed differential equations were constructed according to the theory [15]. The above differential equations depend upon the values of a_1 and a_2. They are intended to obtain the steady-state concentration

$a_2 > \frac{3a_1}{5} - \frac{25}{a_1}$. It was observed in the experimental growth of ZnO nanostructures that the process stopped after a certain period and showed linear behavior [16,17]. The approximate values of the above differential equations were obtained by iterating the following equations:

$$x_{n+1} = x_n + \frac{1}{6}\,(k_1 + 2k_2 + 2k_3 + k_4),$$

$$y_{n+1} = y_n + \frac{1}{6}\,(p_1 + 2p_2 + 2p_3 + p_4),$$

where

$$k_1 = h\, f(x_n, y_n),$$

$$p_1 = h\, g(x_n,\ y_n),$$

$$k_2 = h\, f\left(x_n + \frac{h}{2},\ \ y_n + \frac{k_1}{2}\right),$$

$$p_2 = h\, g\left(x_n + \frac{h}{2},\ \ y_n + \frac{p_1}{2}\right),$$

$$k_3 = h\, f\left(x_n + \frac{h}{2},\ \ y_n + \frac{k_2}{2}\right),$$

$$p_3 = h\, g\left(x_n + \frac{h}{2},\ \ y_n + \frac{p_2}{2}\right),$$

$$k_4 = h\, f(x_n + h,\ \ \ y_n + k_3),$$

$$p_4 = h\, g(x_n + h,\ \ \ y_n + p_3).$$

5. Results and Discussion

The graph in Figure 1 represents the concentrations of OH- obtained from both methods, that is, Euler's method and the RK fourth-order method.

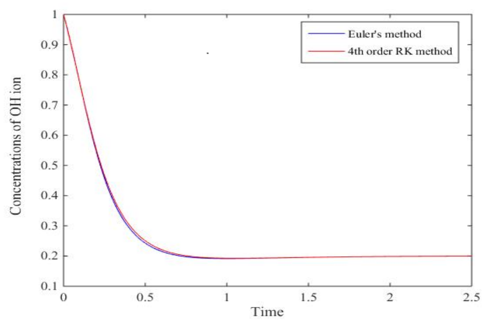

Figure 1. Concentrations of OH ion obtained by Euler’s Method and fourth-

order RK method for the Lengyel-Epstein model [9] with a = 1, b = 12, (x (0), y (0)) = (1, 1).

The curve obtained from both methods showed a steady-state behavior and the formation of OH ions was stopped at 0.2 level of concentration. The exponential decay of the graph depicts that the formation of OH ions decrease over time and tends towards linearity.

5.1 Comparison of Euler's Method and the Fourth-Order RK Method

Figure 1. shows the curve obtained by Euler's method. It shows that after some iterations, the minimum value of the concentration of OH ion is 0.1916. In contrast, the curve obtained by the RK fourth-order method shows that the minimum value may be 0.1926, which is very close to the exact value. Comparing both methods, it was determined that the result of the RK fourth-order method is decidedly better than the result obtained by Euler's method. This is because the error obtained from the RK method at the minimum point is 0.74%, while the error in Euler's method is 0.84%.

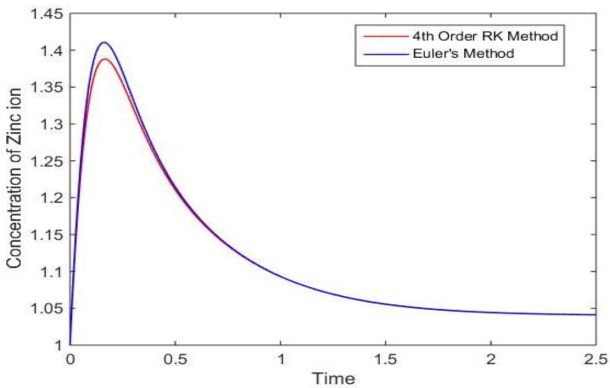

Figure 2. Concentrations of Zinc ion obtained by Euler's method and fourth order RK method using the Lengyel-Epstein model [15] with a = 1, b = 12, (x(0), y(0)) = (1, 1).

The graph in Figure 2. represents the concentrations of Zinc ions obtained from both methods, that is, Euler's method and the RK fourth-order method. The curves obtained from both methods show that exponential decay can be observed in the formation of Zinc ions. Their formation stopped at 1.04 level of concentration and then the graph began to show linear behavior.

Figure 2. shows the curve obtained by Euler's method. It shows that after

some iterations, the maximum value of the concentration of Zinc ion is 1.4108. In contrast, the curve obtained by RK fourth-order method shows that the maximum value is 1.3883 at t=0.16. Comparing both methods, it was determined that RK fourth-order method better predicts the concentration of zinc ions. This is due to the fact that the error obtained from Euler's method at the maximum point is 37.08%, while the error in RK fourth-order method at the maximum level is 34.8%.

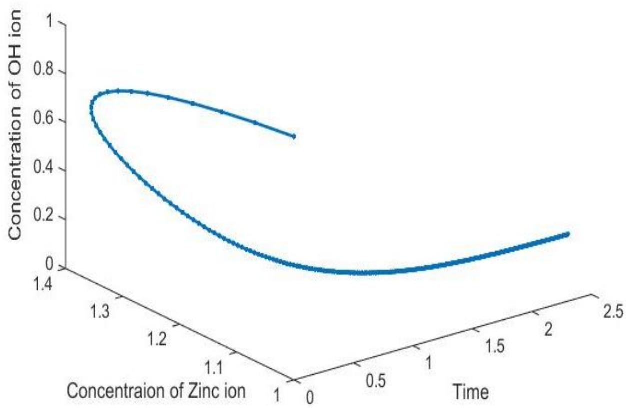

Figure 3. Concentrations of Zinc ion and OH ion using Fourth-Order RK Method. It depicts the concentration of both the ions simultaneously using RK fourth-order method.

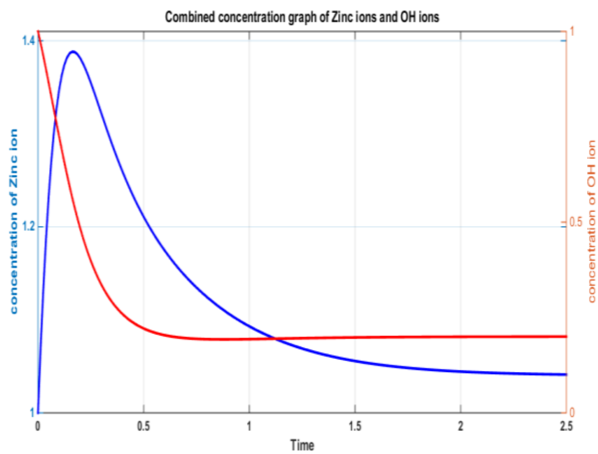

Figure 4. Concentrations of Zinc ion and OH ion using Fourth-Order RK Method

Figure 4. shows the graphs of both concentrations of Zinc and OH ions. Over time, both ions react with each other to form ZnO nanostructures. The model predicts that after a certain time, the growth of ZnO nanostructure stops.

6. Conclusion

The current study recommends the use of fourth-order Runge-Kutta (RK) method in the Lengyel-Epstein reaction model to predict the concentrations of Zinc ions and Hydroxyl ions in the formation of ZnO nanostructures. It also provides a comparison with Euler's method that showed that the rate of convergence of fourth-order RK method is more appropriate than Euler's method using MATLAB. It was determined that the error rate of fourth-order RK method is lower than Euler's method and very close to the experimental result. Hence, it is concluded that Lengyel-Epstein reaction model using the fourth-order RK method provides a strong platform to control and optimize the simulation of growth parameters to achieve one dimensional ZnO nanostructures.

References

[1] Siddiqi KS, Rahman AU, Tajuddin, Husen A. Properties of zinc oxide nanoparticles and their activity against microbes. *Nanoscale Res Lett*. 2018;13(1):1-13. https://doi.org/10.1186/s11671-018-2532-3

[2] Jiang J, Pi J, Cai J. The advancing of zinc oxide nanoparticles for biomedical applications. *Bioinorg Chem Appl*. 2018;2018: e1062562. https://doi.org/10.1155/2018/1062562

[3] Tang E, Cheng G, Ma X, Pang X, Zhao Q. Surface modification of zinc oxide nanoparticle by PMAA and its dispersion in aqueous system. *Appl Surface Sci*. 2006;252(14):5227-5232. https://doi.org/10.1016/j.apsusc.2005.08.004

[4] Fatima K, Khan A, Hussain M. Mathematical modelling of reaction kinematics of one-dimensional zinc oxide nanostructures. *NED Univ J Res*. 2018;15(4):117-122.

[5] Mishra PK, Mishra H, Ekielski A, Talegaonkar S, Vaidya B. Zinc oxide nanoparticles: A promising nanomaterial for biomedical applications. *Drug Discov*. 2017;22(12):1825-1834. https://doi.org/10.1016/j.drudis.2017.08.006

[6] Sabir S, Arshad M, Chaudhari SK. Zinc oxide nanoparticles for

revolutionizing agriculture: synthesis and applications. *Sci World J*. 2014: e925494. https://doi.org/10.1155/2014/925494

[7] Chandiran AK, Abdi-Jalebi M, Nazeeruddin MK, Grätzel M. Analysis of electron transfer properties of ZnO and TiO2 photoanodes for dye-sensitized solar cells. *ACS nano*. 2014;8(3):2261-2268. https://doi.org/10.1021/nn405535j

[8] Bai X, Wang L, Zong R, Lv Y, Sun Y, Zhu Y. Performance enhancement of ZnO photocatalyst via synergic effect of surface oxygen defect and graphene hybridization. *Langmuir*. 2013;29(9):3097-3105. https://doi.org/10.1021/la4001768

[9] Hatamie A, Khan A, Golabi M, et al. Zinc oxide nanostructure-modified textile and its application to biosensing, photocatalysis, and as antibacterial material. *Langmuir*. 2015;31(39):10913-10921. https://doi.org/10.1021/acs.langmuir.5b02341

[10] Fathoni M F, Wuryandari AI. Comparison between Euler, Heun, Runge-Kutta and Adams-Bashforth-Moulton integration methods in the particle dynamic simulation. Paper presentation at; 4th International Conference on Interactive Digital Media (ICIDM); December 1-5, 2015; Bandung, Indonesia; https://doi.org/10.1109/ IDM.2015.7516314

[11] Khan A, Hussain M, Abbasi MA, Ibupoto ZH, Nur O, Willander M. Analysis of junction properties of gold–zinc oxide nanorods-based Schottky diode by means of frequency dependent electrical characterization on textile. *J Mater Sci*. 2014;49(9):3434-3441. https://doi.org/10.1007/s10853-014-8053-2

[12] Qiu Y, Zhang H, Hu L, et al. Flexible piezoelectric nanogenerators based on ZnO nanorods grown on common paper substrates. *Nanoscale*. 2012;4(20):6568-6573. https://doi.org/10.1039/ c2nr31031g

[13] Lee CY, Wang JY, Chou Y, et al. White-light electroluminescence from ZnO nanorods/polyfluorene by solution-based growth. Nanotechnology. 2009;20(42): e425202.

[14] Greene LE, Yuhas BD, Law M, Zitoun,D, Yang P. Solution-grown zinc oxide nanowires. *Inorg Chem*. 2006;45(19):7535-7543. https://doi.org/10.1021/ic0601900

[15] Zafar ZUA. Fractional order Lengyel–Epstein chemical reaction model. *Comp. Appl. Math*. 2019;38: e131. https://doi.org/10.1007/

s40314-019-0887-4

[16] Fatima K, Ali B, Qari R, Khan AA, Arshad M. Impact Estimation of Offshore Floating Solar Parks on Algae using Ordinary Differential Equations. *J Indep Stud Res Comput*. 2021;19(2):42-48. https://doi.org/10.31645/JISRC.38.19.2.6

[17] Ali B, Khan AA, Siddique I, Bhutta JA, Israr M. Fast track implementation of energy management system 2018 using sequential approach. Paper presented at; IEEE 23rd International Multitopic Conference (INMIC); November 5-7, 2020; Bahawalpur, Pakistan. https://doi.org/10.1109/INMIC50486.2020.9318204